iScience

CellPress
OPEN ACCESS

Article

Detecting time-evolving phenotypic components of adverse reactions against BNT162b2 SARS-CoV-2 vaccine via non-negative tensor factorization

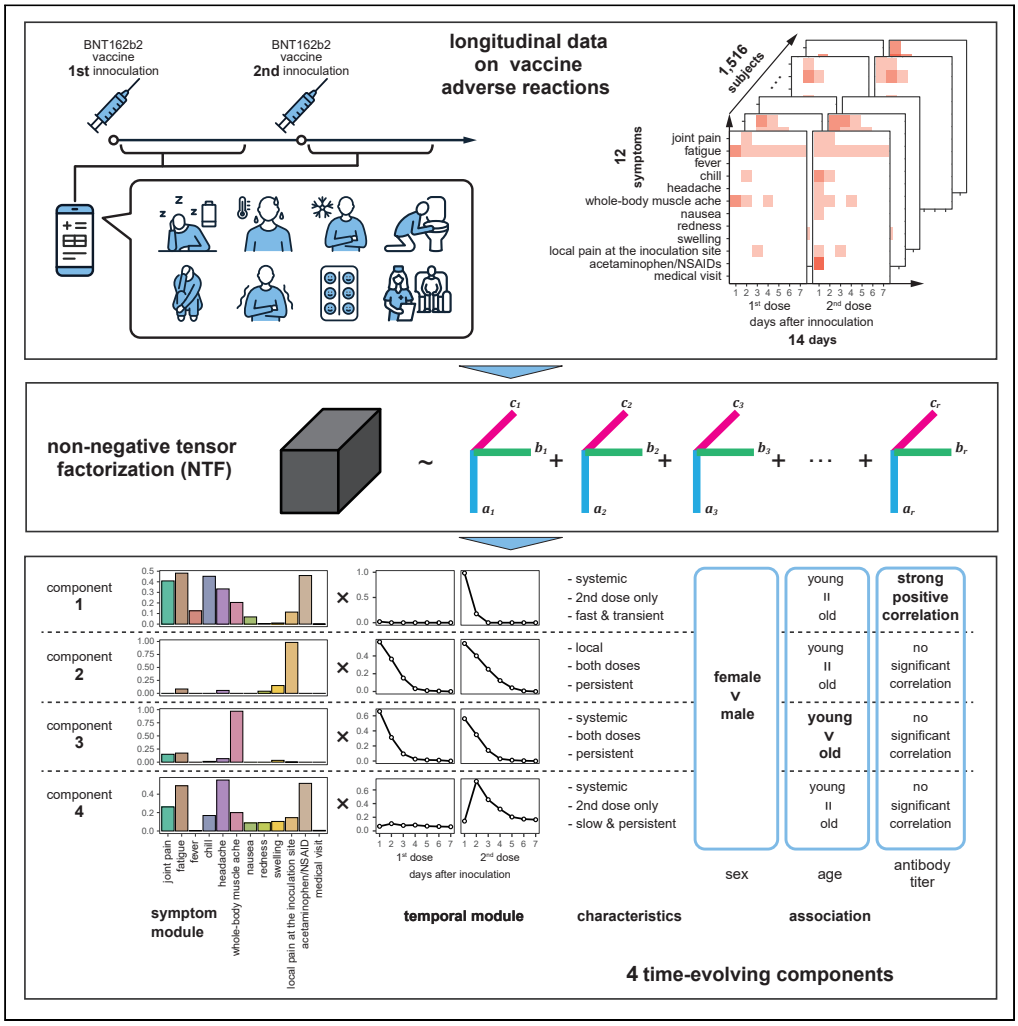

Kei Ikeda, Taka-Aki Nakada, Takahiro Kageyama, ..., Koki Tsuyuzaki, Hiroshi Nakajima, Eiryo Kawakami

nakajimh@faculty.chiba-u.jp (H.N.)
eiryo.kawakami@chiba-u.jp (E.K.)

Highlights

Tensor factorization identified 4 components that explain vaccine adverse reactions

These components were differently associated with background factors

Only 1 component was significantly associated with post-vaccine antibody titer

These methods and results will inform future studies on vaccine safety and efficacy

Ikeda et al., iScience 25, 105237
October 21, 2022
https://doi.org/10.1016/j.isci.2022.105237

iScience

CellPress
OPEN ACCESS

Article

Detecting time-evolving phenotypic components of adverse reactions against BNT162b2 SARS-CoV-2 vaccine via non-negative tensor factorization

Kei Ikeda,[1,18] Taka-Aki Nakada,[2,18] Takahiro Kageyama,[1,18] Shigeru Tanaka,[1] Naoki Yoshida,[3] Tetsuo Ishikawa,[4] Yuki Goshima,[4] Natsuko Otaki,[3] Shingo Iwami,[5,6,7,8,9,10] Teppei Shimamura,[11] Toshibumi Taniguchi,[12] Hidetoshi Igari,[12,13] Hideki Hanaoka,[14] Koutaro Yokote,[15] Koki Tsuyuzaki,[16] Hiroshi Nakajima,[1,13,*] and Eiryo Kawakami[3,4,9,17,19,*]

SUMMARY

Symptoms of adverse reactions to vaccines evolve over time, but traditional studies have focused only on the frequency and intensity of symptoms. Here, we attempt to extract the dynamic changes in vaccine adverse reaction symptoms as a small number of interpretable components by using non-negative tensor factorization. We recruited healthcare workers who received two doses of the BNT162b2 mRNA COVID-19 vaccine at Chiba University Hospital and collected information on adverse reactions using a smartphone/web-based platform. We analyzed the adverse-reaction data after each dose obtained for 1,516 participants who received two doses of vaccine. The non-negative tensor factorization revealed four time-evolving components that represent typical temporal patterns of adverse reactions for both doses. These components were differently associated with background factors and post-vaccine antibody titers. These results demonstrate that complex adverse reactions against vaccines can be explained by a limited number of time-evolving components identified by tensor factorization.

INTRODUCTION

While no definitive post-onset treatment for COVID-19 has yet been established, vaccination against SARS-CoV-2 is the most promising strategy to prevent the spread of COVID-19. Several trials, including the phase 3 trials that provided the basis for emergency use authorization, have shown that the SARS-CoV-2 vaccines reduce the infection, severe disease, and death of COVID-19 (Baden et al., 2021; Dagan et al., 2021; Frenck et al., 2021; Haas et al., 2021; Polack et al., 2020; Voysey et al., 2021). On the other hand, the SARS-CoV-2 vaccines cause a wide range of adverse reactions including injection site events and systemic responses (Baden et al., 2021; Polack et al., 2020; Sadoff et al., 2021; Voysey et al., 2021). Although the incidence of life-threatening serious adverse events was low, systemic reactions such as headache and fever have been reported to occur with a frequency of 60%-80% (Baden et al., 2021; Polack et al., 2020; Sadoff et al., 2021). As booster and/or routine vaccinations are being considered for long-term protection and response to mutant viruses, the adverse reactions that affect daily life are a matter of social concern. A precise characterization of adverse reactions may facilitate the development of safer vaccines and the establishment of safer vaccination schemes.

A data-driven approach to characterize complex phenotypes such as adverse reactions is to break them down into a small number of patterns. Topic modeling approaches, such as non-negative matrix factorization (NMF) and Latent Dirichlet Allocation (LDA), have been applied to identify latent symptom patterns (i.e., subphenotypes) from electronic health record (EHR) data (Huang et al., 2015; Lu et al., 2016; Pivovarov et al., 2015; Zhao et al., 2019a). Describing disease as an ensemble of subphenotypes helps us to investigate associations with clinical outcomes and to generate testable hypotheses about the underlying mechanisms.

[1]Department of Allergy and Clinical Immunology, Graduate School of Medicine, Chiba University, Chiba 260-8670, Japan

[2]Department of Emergency and Critical Care Medicine, Graduate School of Medicine, Chiba University, Chiba 260-8670, Japan

[3]Artificial Intelligence Medicine, Graduate School of Medicine, Chiba University, Chiba 260-8670, Japan

[4]Advanced Data Science Project (ADSP), RIKEN Information R&D and Strategy Headquarters, Yokohama, Kanagawa 230-0045, Japan

[5]Interdisciplinary Biology Laboratory (iBLab), Division of Biological Science, Graduate School of Science, Nagoya University, Nagoya, Aichi 464-8602, Japan

[6]Institute of Mathematics for Industry, Kyushu University, Fukuoka 819-0395, Japan

[7]Institute for the Advanced Study of Human Biology (ASHBi), Kyoto University, Sakyo Ward, Kyoto 606-8501, Japan

[8]Interdisciplinary Theoretical and Mathematical Sciences Program (iTHEMS), RIKEN, Wako, Saitama 351-0198, Japan

[9]NEXT-Ganken Program, Japanese Foundation for Cancer Research (JFCR), Koto Ward, Tokyo 135-8550, Japan

[10]Science Groove Inc., Fukuoka 810-0041, Japan

[11]Division of Systems Biology, Nagoya University Graduate

Continued

In identifying the subphenotypes of vaccine adverse reactions, it is important to note that symptoms evolve and progress over time as a series of immune responses. However, conventional studies on vaccine adverse reactions have focused mainly on the frequency and intensity of symptoms and the temporal progression of symptoms is only presented as a population average. Different timing of occurrence of the same symptom may reflect different immune responses, but information on frequency and intensity does not allow us to distinguish the difference.

In this study, we extract time-evolving subphenotypes of vaccine adverse reactions by using non-negative tensor factorization (NTF), one of the topic modeling approaches (Luo et al., 2017). Tensor decomposition has been shown to be useful in integrating information from different modalities and interpreting complex information, such as analyzing gene expression patterns considering 3D anatomical structures (Ji, 2011) and extracting relationships between genes and regulatory transcription factors (Roy et al., 2014). Tensor decomposition has also been applied to Electroencephalogram (EEG) data to analyze epileptic seizures (Acar et al., 2007) and to fMRI data to classify cognitive states (Batmanghelich et al., 2011). In recent years, tensor decomposition has been applied to longitudinal EHR data to extract time-evolving phenotypes of diseases (Perros et al., 2019; Zhao et al., 2019b). We collected information on adverse reactions against BNT162b2 mRNA COVID-19 vaccine every day from day 1 to day 7 after each dose of vaccination using a smartphone/web-based platform (Yamada et al., 2019), which is represented as a third-order tensor consisting of three axes: symptoms, time, and subjects. A tensor-factorization model can identify the co-occurring symptoms as subphenotypes, describe their temporal progression, and obtain individual intensities of subphenotypes. We demonstrate that diverse and complex adverse reactions to the BNT162b2 vaccine can be decomposed into four time-evolving components. We also show that these components are differently associated with post-vaccine antibody titers and other external information such as immediate reactions and background factors.

RESULTS

Uncovering time-evolving subphenotypes of adverse reactions by negative tensor factorization

We applied NTF to the adverse-reaction data to extract time-evolving subphenotypes. The data on adverse reactions are represented as a 3-way array consisting of three axes: symptoms, time, and subjects (*S* columns, *T* rows, and *N* slices in Figure 1, respectively). NTF aims to decompose such apparently complex data into a sum of a small number of latent components. Each latent component is expressed as the outer product of symptom module $\boldsymbol{a}_k$, temporal module $\boldsymbol{b}_k$, and subject module $\boldsymbol{c}_k$, indicating what types of symptoms occur at what times and in what populations (Figure 1). To select the optimal number of the latent components (*r* in Figure 1), we repeatedly decomposed the original data, each with a random 20% of elements deleted, into a different number of components and calculated reconstruction loss (Lin and Boutros, 2020). The median reconstruction error was the smallest when we decomposed the data into four components (Figure S2).

Thus, we extracted four components, consisting of symptom modules, temporal modules, and subject modules (Figure 2A). Component 1 showed diverse systemic symptoms almost exclusively on day 1 after the second dose. Components 2 and 3 shared a similar time course over the two doses, but component 2 was a local event characterized by local pain at the inoculation site, while the main symptom of component 3 was whole-body muscle ache, a systemic response. Similar to component 1, component 4 was characterized by a wide range of systemic symptoms but peaked on day 2 after the second dose.

As shown in the subject module (Figure 2A), component 2 was the most frequent, with more than half of the subjects showing the pattern (1,029 subjects with a $\boldsymbol{c}_1$ score >1.0). Components 1 and 3 were present in about one-third of subjects (746 and 603 subjects with a score >1.0, respectively), and component 4 was the least frequent, with 407 subjects showing a $\boldsymbol{c}_4$ score >1.0.

The study subjects were divided into three major groups when stratified by hierarchical clustering based on these four component scores for subjects (Figure 2B). Group 1 had high component 1 and 4 scores together with the other scores and was considered to represent subjects with severe adverse reactions. Group 2 had high component 1 scores but low component 4 scores and can be interpreted as a group with moderate adverse reactions. Group 3 was mostly mild cases that showed few symptoms except for local pain at the inoculation site or whole-body muscle ache represented by components 2 and 3.

School of Medicine, Nagoya, Aichi 466-8550, Japan

[12]Department of Infectious Diseases, Chiba University Hospital, Chiba University, Chiba 260-8670, Japan

[13]Chiba University Hospital COVID-19 Vaccine Center, Chiba University, Chiba 260-8670, Japan

[14]Clinical Research Centre, Chiba University Hospital, Chiba University, Chiba 260-8670, Japan

[15]Department of Endocrinology, Hematology and Gerontology, Graduate School of Medicine, Chiba University, Chiba 260-8670, Japan

[16]Laboratory for Bioinformatics Research, RIKEN Center for Biosystems Dynamics Research, Wako, Saitama 351-0198, Japan

[17]Institute for Advanced Academic Research (IAAR), Chiba University, Chiba 260-8670, Japan

[18]These authors contributed equally

[19]Lead contact

*Correspondence: nakajimh@faculty.chiba-u.jp (H.N.), eiryo.kawakami@chiba-u.jp (E.K.)

https://doi.org/10.1016/j.isci.2022.105237

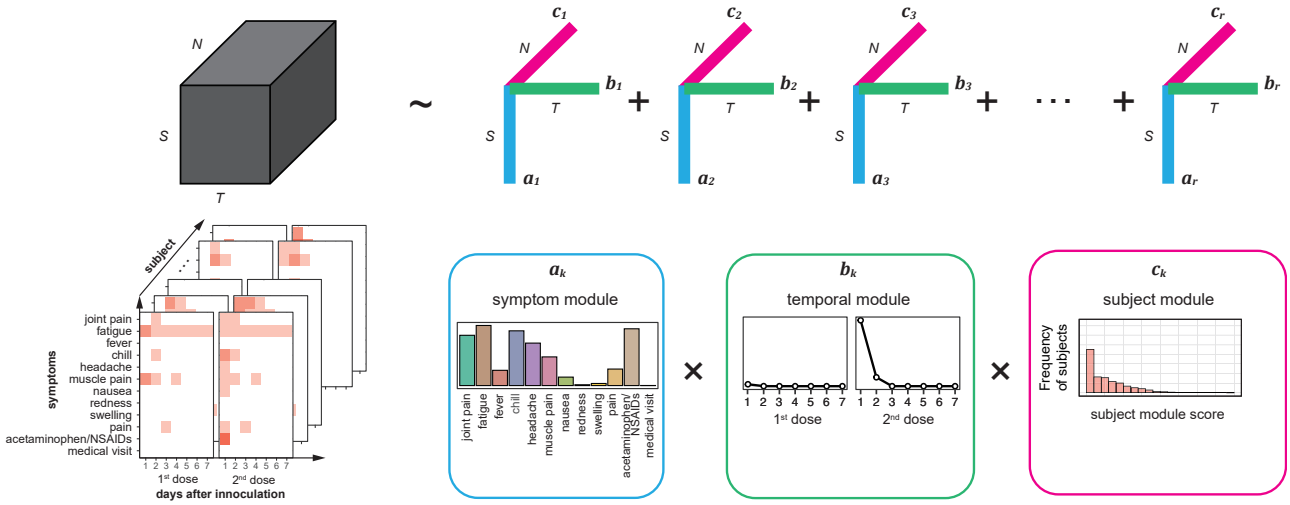

Figure 1. Schematic of tensor factorization of adverse reactions against two doses of BNT162b vaccine

The time-series data for vaccine adverse reactions can be represented as a 3D tensor consisting of three indices: symptoms (*S*), time (*T*), and subjects (*N*). Tensor factorization aims to approximate the 3D tensor by a sum of a small number of latent components. Each component is represented by the outer products of the symptom, time, and subject modules. The symptom module indicates what symptoms are included in the component, the time module indicates at what timing the component appears, and the subject module indicates in which subjects the component appears.

Validation of negative tensor factorization

To evaluate whether the components extracted by NTF reflect the characteristics of the original data, we compared the data reconstructed from the components with the original data. The reconstruction error for the whole data evaluated by MSE was 0.060 and the coefficient of determination R^2 was 0.53, indicating that most of the data were well explained by the sum of the components obtained from the NTF.

To investigate the impact of considering time dependence on decomposition, we then applied NMF, as a comparative method of NTF, to the adverse-reaction data at each time point independently. The optimal number of latent components of NMF determined by the masking approach was one except for day 5 after the second dose, which had two components (Figure S3). The NMF components represent the most typical phenotypic pattern of the day, but they do not capture the heterogeneity of phenotypes or the association of components between time points. The reconstruction error evaluated by MSE was 0.093 and R^2 was 0.31 for the NMF model, showing that the NTF model fits better with the data. Thus, the NTF could precisely extract the dynamic changes in phenotypes as a small number of interpretable components, which are difficult to extract by independent analysis of each time slice.

We further examined how the pattern of adverse reactions was represented by the tensor components for each subject. Four representative subjects are shown in Figure 3A. Subject #27 was a very mild case, presenting with whole-body muscle ache on day 1 after both the first and second inoculations, and fatigue, chill, headache, and use of acetaminophen/NSAID after the second dose only. This pattern is represented by the sum of components 1 and 3. Subject #521 had similar symptoms but also showed local pain at the inoculation site after both inoculations. In this case, the symptoms are mainly represented as the sum of components 1 and 2. Subject #79 was a case with missing values, who did not respond on day 5 after the second inoculation. The NTF could accommodate missing data with mask property and reconstruct the data by estimating the values that would have been there. Subject #329 was a rather unique case, with severe and widespread symptoms that persisted for seven days after both the first and second doses. In this case, component 4 showed a very high value. Taken together, although the original symptom patterns were accurately reconstructed based on the tensor components in most subjects, there were some exceptions.

When we sorted the 1,516 subjects by reconstruction error, only nine subjects, including subject #329, had very high reconstruction errors with MSE>0.4 (Figure 3B). All these nine subjects had persistent severe symptoms, which would be difficult to be adequately represented by the four tensor components because all these components had a peak on day 2 or earlier. Component 4 score for subjects was significantly

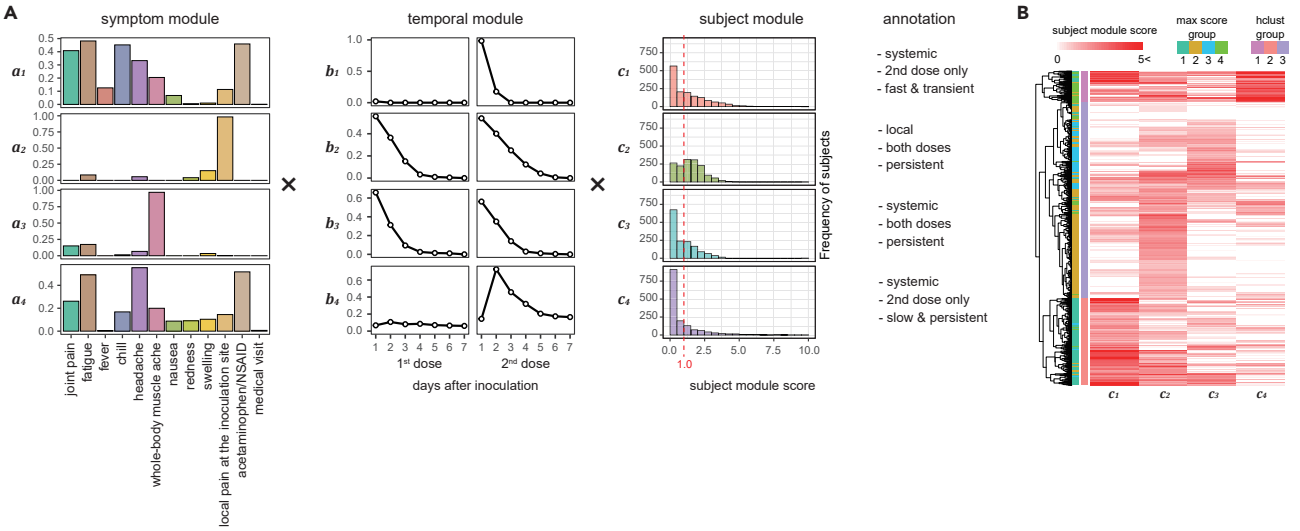

Figure 2. Four tensor components identified and corresponding modules

(A) The tensor factorization yielded four components corresponding to the major patterns of adverse reactions. Each component is represented by the outer product of the modules in a horizontal row. For example, component 1 consists of a_1 as the symptom module, b_1 as the temporal module and c_1 as the subject module. The *y* axis for symptom and temporal modules represents the weights of modules normalized so that their L2-norms are equal to 1.

(B) Stratification of subjects based on subject module scores (c_1, c_2, c_3, and c_4). Subjects are clustered into three major groups by hierarchical clustering using Euclidean distance based on the subject module scores. Clusters based on maximum module scores are also in the side bar.

associated with reconstruction errors (Table S3), suggesting that atypically severe, widespread, and persistent adverse reactions could not be solely explained by the four components.

Association of tensor components with immediate reactions

Next, we investigated how the tensor components were associated with immediate reactions on day 0. Immediate reactions rarely occurred after the first dose, and the correlation coefficient could not be calculated for some symptoms (gray area in Figure 4A), and no significant correlations were detected for the first dose (Figure 4A, left panel). In contrast, some immediate reactions after the second dose were strongly associated with the tensor components of adverse reactions: redness at the inoculation site was strongly correlated with components 1 and 4; itching with component 4; and nausea with components 1 and 4 (Figure 4A, right panel). Components 2 and 3 showed no significant association with immediate reactions.

Association of tensor components with background factors

We then examined the relationships of the tensor components with background factors (Figures 4B-4E). A history of adverse reactions to other vaccines was positively associated with component 4 score for subjects. A history of contact with patients with COVID-19 was also significantly associated with adverse reactions; no contact with patients with COVID-19 at all was negatively associated with component 3 score for subjects. A history of flu symptoms within a year had a positive association with component 4 score for subjects. Regarding habits, no drinking had a positive association with component 4 score for subjects. Occupations were also significantly associated with adverse reactions with doctors negatively associated with components 1, 3, and 4 scores for subjects, and nurses positively associated with components 1, 2, and 4 scores for subjects. We should note that occupation is strongly confounded with sex. Doctors had about three times as many males as females, and conversely, nurses had only about one-10th as many males as females (Table S4).

Regarding comorbidities and current medications, malignancy was positively associated with component 4 score for subjects. Autoimmune diseases showed positive associations with component 4 score for subjects. Inhaled and oral corticosteroid and anti-allergic drug were positively associated with component 4 score for subjects, and thyroid drug was also positively associated with component 1 score for subjects.

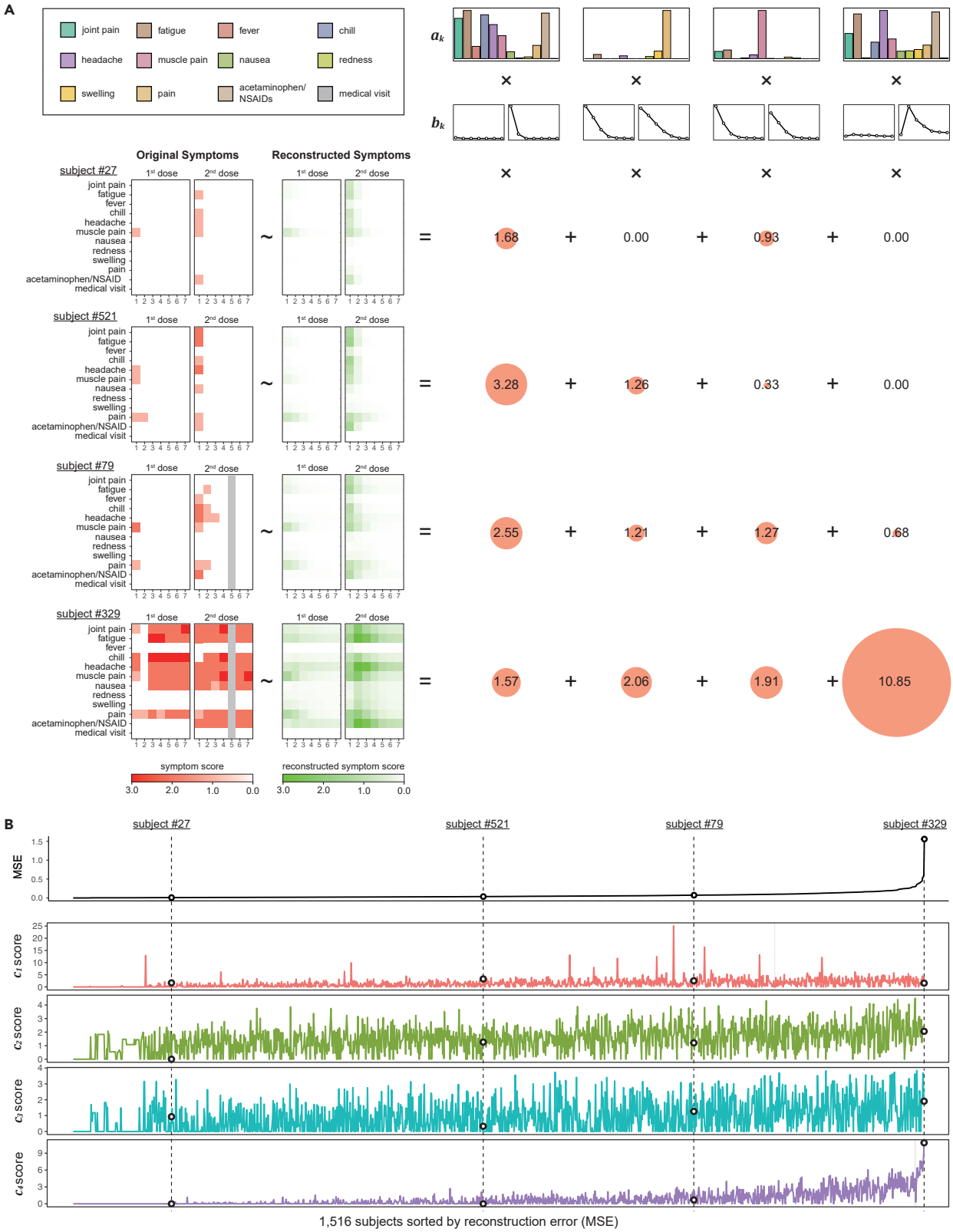
A
joint pain
fatigue
fever
chill
headache
muscle pain
nausea
redness
swelling
pain
acetaminophen/ NSAIDs
medical visit
a_k
b_k
Original Symptoms
Reconstructed Symptoms
subject #27
subject #521
subject #79
subject #329
1st dose
2nd dose
1.68
0.00
0.93
0.00
3.28
1.26
0.33
0.00
2.55
1.21
1.27
0.68
1.57
2.06
1.91
10.85
symptom score
reconstructed symptom score
B
MSE
c_1 score
c_2 score
c_3 score
c_4 score
1,516 subjects sorted by reconstruction error (MSE)

Figure 3. Representative cases and validation of tensor components

(A) Four representative cases illustrating how actual symptoms are approximated by the sum of the four tensor components. In each case, the score of the subject module is shown as a number with a red circle representing the amplitude of the score. The symptoms reconstructed by the sum of the components are shown as a green heatmap to the right of the original score.

(B) Subjects sorted by reconstruction error (MSE) and corresponding subject module scores. The tensor component scores for the 1,516 subjects are sorted in the same order as the MSE graph, with a vertical column representing the MSE and tensor component scores for the same subject. The four representative subjects appearing in (A) are indicated by dotted lines and open circles.

Women scored significantly higher on all components than men (Figure 4E and Table S5). The association between age and the tensor component was different for each component. For component 3, the 40 and 50s subjects scored significantly lower. Components 1, 2, and 4 scores for subjects were not significantly related to age.

Association of tensor components with antibody titers

We have previously reported that post-vaccination anti-SARS-CoV-2S antibody titers were affected by the time from second dose to the antibody test, age, sex, the interval between the first and second inoculation, drinking habits, and comorbidities and their medications (Kageyama et al., 2021). Using a generalized additive model that considers the influence of these factors as covariates, we assessed the impact of the tensor components on the post-vaccination antibody titer. We found a strong positive correlation between component 1 score for subjects and the post-vaccination antibody titer, which was similar for both women and men (Figure 4F and Table 1). However, no significant associations were found for the other three components.

Predictability of adverse reactions and antibody titers

Several significant associations between background factors and tensor components of adverse reactions led us to predict adverse reactions based on background factors. To account for nonlinearities and interactions among background factors, we used a random forest (RF) classifier to predict whether each component score for subjects would exceed a threshold of 1.0. For components 1 and 4 scores for subjects, the area under the receiver operating characteristics curve (AUC), a measure of predictive accuracy, was around 0.65, indicating partial predictability (Figure 5A). On the other hand, the AUC for the scores of components 2 and 3 scores for subjects was low, especially for component 2, AUC = 0.504, indicating almost no predictability. We then assessed the contribution of each background factor to prediction using permutation importance. Factors that have shown significant associations in statistical association analyses (Figures 4A–4E), including age and sex, were identified as important predictors (Figure 5B).

Finally, we predicted antibody titers from background factors and tensor component scores for subjects. Because of the nonlinearity of the antibody titer, it was difficult to predict the value of antibody titer as a regression problem. Therefore, we set six thresholds of antibody titer (10^8, 10^9, 10^{10}, 10^{11}, 10^{12}, and 10^{13}) and predicted antibody titers as a binary classification problem with RF, whether the antibody titer exceeds each threshold (Figure 5C). The AUCs were 0.645-0.867 for the respective antibody titer thresholds, suggesting the partial predictability of antibody titer (Figure 5D). When the contribution of each variable to prediction was examined by permutation importance, subject scores of the tensor component were extracted as important predictors, in addition to time from second dose to antibody test, interval between the first and second inoculation, acetaminophen/NSAID-intake, and age (Figure 5E). The $\boldsymbol{c}_1$ subject score was important for prediction using 10^{10}, 10^{11}, and 10^{12} threshold, consistent with $\boldsymbol{c}_1$ score being significantly associated with antibody titers.

DISCUSSION

In this study, we decomposed longitudinal data on adverse reactions after two doses of the SARS-CoV-2 vaccine into four time-evolving components by NTF. Of these four components, one represents inoculation site events and other three represent systemic responses, suggesting that the systemic adverse reactions, which have been treated collectively, consist of different immunological elements. Each component was associated differently with responses immediately after vaccination and with background information such as age, sex, and comorbidities. Furthermore, we found that only component 1, which corresponds to the diverse systemic responses on day 1 after the second inoculation, was positively correlated with post-vaccination antibody titer.

One of the main technical challenges in this study is the rank optimization in the NTF. In unsupervised learning, the number of elements to be decomposed (i.e., rank) must be specified in advance. Several methods using coherence, which means whether a decomposed component represents a meaningful

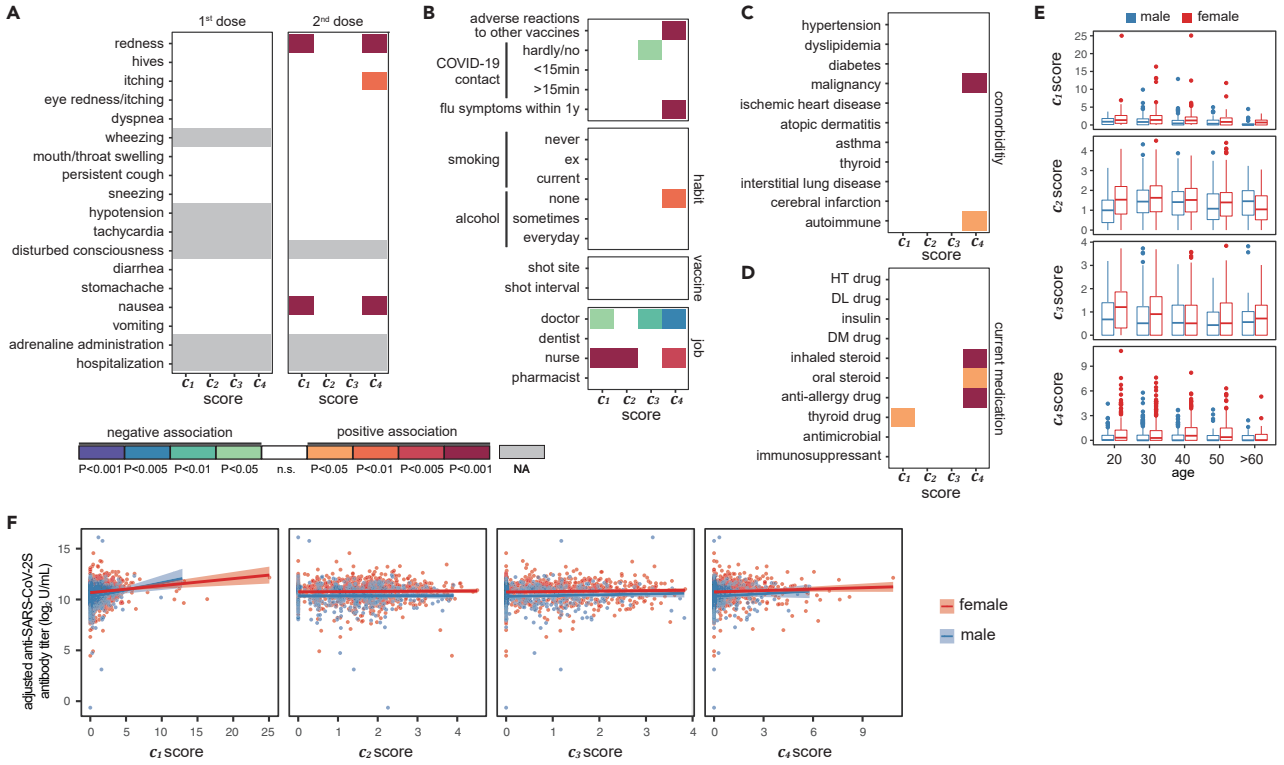

Figure 4. Associations of tensor components with immediate reactions, background information, and antibody titers

(A–D) Heatmaps of statistically significant associations of tensor component scores for subjects with immediate reactions on the day of vaccination (A), background factors such as COVID-19 contact, habits, and jobs (B), comorbidities (C), and current medications (D). Associations with the immediate reactions were assessed using Spearman's rank correlation and other associations were assessed using the Tweedie generalized linear model. FDR-corrected p values less than 0.05 were considered significant.

(E) Associations of tensor components scores for subjects with sex and age.

(F) Associations between tensor component scores for subjects and post-vaccination anti-SARS-CoV-2S antibody titers. In this plot, antibody titers were adjusted to the standard conditions of interval to test (days) = 21, inoculation interval (days) = 21, age (year-old) = 40, alcohol = none, immunosuppressant = none, glucocorticoid = none, anti-allergic drug = none, and post COVID-19 infection = none by using a generalized additive model. The shaded area represents the 95% confidence interval of the regression line.

concept, as a metric for factorization have been proposed in topic modeling (Chang et al., 2009; Lau et al., 2014; Newman et al., 2010; Stevens et al., 2012; Zhao et al., 2019b). However, as this study dealt with ordinal measures of symptom severity rather than binary topics, it was difficult to use the coherence within topics as a metric. There are some ad hoc approaches for the rank optimization in NTF and NMF including the elbow method and similar techniques (Fanaee-T and Gama, 2016; Gaujoux and Seoighe, 2010; Lin and Boutros, 2020) but such methods should subjectively select the optimal rank. When we calculated the reconstruction error for all elements, not just the masked elements, the reconstruction error decreased monotonically as the rank increased (Figure S4). The decrease was gradual, and it was difficult to determine the elbow. Instead, we introduced a masking approach that finds a suitable rank to remove noise and restore the original data. An optimal rank that properly captures the dependencies among elements is expected to give the smallest error rate in imputing the missing values introduced as noise. The noise required for this approach is as simple as randomly masking elements, and there is no need to assume a noise distribution. The only parameter that has to be set is the percentage of elements to be masked as noise. When we varied the percentage of masked elements to 5%, 10%, 20%, and 30%, the rank showing the smallest reconstruction error in the adverse reaction data was always four, confirming that the estimation of the optimal rank is not affected much by the percentage of masked elements (Figure S5). As shown in Figures S2 and S4, the reconstruction errors take large values in some decompositions and show a long-tail distribution. Therefore, we adopted the median rather than the mean of the reconstruction error as the measure of rank optimization. The simple and intuitive masking approach will have broad utility in any unsupervised learning method with the capability of missing value imputation.

Table 1. Generalized additive models to evaluate the association between adverse reaction component scores and post-vaccination antibody titers

component	population	coefficient	p value	FDR
c_1	all	**0.08**	7.2E-7	**8.6E-6**
	female	**0.066**	0.00015	**0.0016**
	male	**0.13**	0.00042	**0.0042**
c_2	all	0.025	0.42	1
	female	0.024	0.50	1
	male	0.031	0.58	1
c_3	all	0.037	0.23	1
	female	0.033	0.33	1
	male	0.055	0.36	1
c_4	all	0.052	0.013	0.24
	female	0.042	0.084	0.68
	male	0.060	0.31	1

bold: significant association (FDR <0.05).

Although it is beyond the scope of this study, we believe that formalizing biomedical data as a tensor and performing tensor decomposition are highly expandable and promising in several directions. For example, the Tucker version of non-negative tensor decomposition (NTD) can be formalized by setting the different ranks for each module (Cichocki et al., 2009). Although the CP decomposition used in this study has an advantage in simplified interpretation, the Tucker decomposition may provide a more flexible and realistic decomposition (Luo et al., 2017). To evaluate reconstruction errors, we can try not only Euclidean distance assuming the Gaussian distribution, but also Kullback-Leibler (KL)-divergence assuming the Poisson distribution, Itakura-Saito (IS)-divergence assuming the Gamma distribution, and many other divergences (Cichocki et al., 2009). These family divergences are referred to as Alpha-Beta-divergences (AB-divergences) and are parameterized by the two parameters (Cichocki et al., 2011). As IS-divergence has been reported to perform well in acoustic data analysis (Févotte et al., 2009), the AB-divergences will allow us to deal with various types of data obtained in biomedical research. Coupled matrix and tensor factorization (CMTF, Acar et al., 2013) can decompose matrices and tensors in a coupled manner. In biomedical research, where incomplete and heterogeneous datasets are obtained, it will become increasingly important to use the joint analysis as CMTF to clarify relationships between heterogeneous datasets and to compensate for missing information. Furthermore, the current NTF does not consider the order of time and cannot characterize temporal interactions. Incorporating architectures such as long short-term memory (LSTM) to account for temporal interactions would be one direction to generalize NTF (Wu et al., 2019).

The four tensor components of adverse reactions provide us with implications of the immune responses against the SARS-CoV-2 vaccine. Components 2 and 3, which were characterized by local inoculation-site pain and whole-body muscle ache, respectively, are likely to reflect innate immune responses because they showed the same dynamics after the first and second dose and were not associated with antibody responses. The innate immune response to vaccines has been known to have two routes (Hervé et al., 2019): the first route is called the neural route, in which immune cells stimulate nociceptors with cytokines and direct contact, causing local pain (Ren and Dubner, 2010); the second route is called the humoral route, in which cytokines produced by immune cells leak into the circulatory system and act on the CNS, causing systemic fever, headache, and whole-body muscle ache (Saper et al., 2012; Vasilache et al., 2015). Component 2 identified in our study includes local pain at the inoculation site as well as local symptoms such as redness and swelling, suggesting that it corresponds to the neural route. Component 3 includes whole-body muscle ache as well as joint pain and fatigue, which would correspond to the humoral route. The fact that there was little overlap between the subject populations showing components 2 and 3 (Figure 2B), and that only component 3 showed a significant negative correlation with age, suggests that the two innate immune routes are independently regulated.

Components 1 and 4 share the common feature that diverse systemic symptoms are boosted only after the second dose, which may reflect acquired immune responses. It is well known that T cells and B cells contribute to the formation of immune memory in acquired immunity (Lauvau and Goriely, 2016). A few

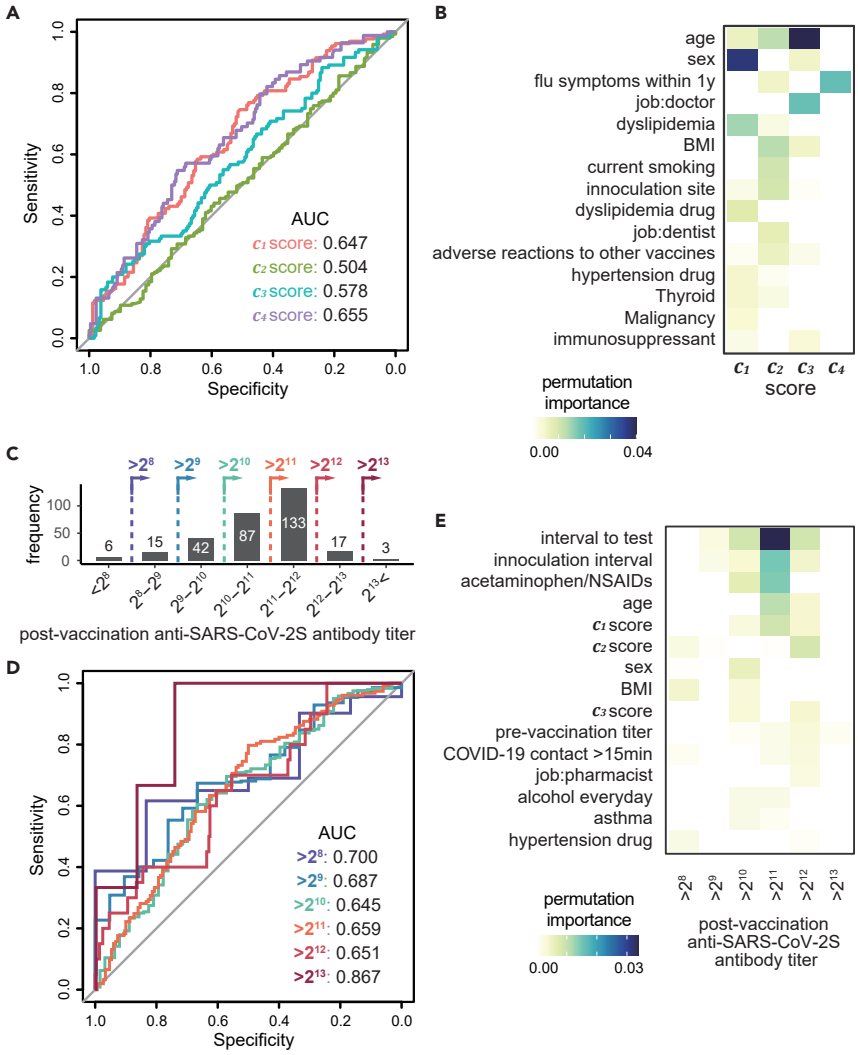

Figure 5. Predictions of tensor components and antibody titers using random forest classifiers

(A) Receiver Operating Characteristic (ROC) curves for the validation dataset in predicting whether each component score for subjects would exceed a threshold of 1.0.

(B) Contribution of each background factor to prediction using permutation importance. Variables are sorted by the maximum permutation importance score for the four prediction models, and a heatmap shows the importance of the top 15 variables.

(C) Distribution of post-vaccination anti-SARS-CoV-2S antibody titer. We set six thresholds of antibody titer (10^8, 10^9, 10^{10}, 10^{11}, 10^{12}, and 10^{13}) and predicted antibody titers as a binary classification problem.

(D) ROC curves for the validation dataset in predicting antibody titers from background factors and tensor component scores for subjects.

(E) Contribution of each background factor to antibody titer prediction using permutation importance. Variables are sorted by the maximum permutation importance score for the six prediction models, and a heatmap shows the importance of the top 15 variables.

percent of T cells and B cells sensitized to an antigen differentiate into long-lived memory cells and induce a rapid and efficient immune response when the same antigen appears again (Cooper and Alder, 2006; Parish and Kaech, 2009). The response enhanced by acquired immunity is suppressed by CD4 T cells and regulatory T cells, thus preventing harmful immunopathology (Palm and Medzhitov, 2007). Component 1 of the vaccine adverse reaction represents a rapid and strong immune response boosted by adaptive immunity. The fact that only component 1 was strongly and positively associated with post-vaccination antibody titers also supports this hypothesis. On the other hand, component 4, compared with component 1, was characterized by a slower peak and more persistent symptoms (Figure 2A) and occurred in a smaller

number of cases, particularly atypical ones (Figures 2 and 3B). Subjects with a strong component 4 were more likely to have had adverse reactions to other vaccines (Figure 4B), and had a higher rate of malignancies, autoimmune diseases, and steroid administration (Figures 4C and 4D). This suggests that component 4 arises in the context of the dysregulation of acquired immunity. One of the directions for the development of safer vaccines will be to suppress the innate immune response and dysregulation of acquired immunity that may lead to harmful immunopathology, while maintaining the activation of memory B cells that lead to antibody production.

Prediction of adverse reactions based on background factors revealed that adverse reaction components 1 and 4 were partially predictable. The predictability of these systemic adverse reactions may lead to advance prescription of acetaminophen/NSAIDs for high-risk population. Antibody titers were also partially predictable from background factors and adverse reactions. As it is not practical to measure antibody titers at a fixed time for all vaccinated populations, the antibody titer prediction model developed in this study can be used to screen populations in which antibody titers may not rise sufficiently and to recommend additional vaccinations.

In conclusion, we demonstrated that tensor factorization was able to summarize complex data on vaccine-induced adverse reactions into a limited number of time-evolving components that could differentiate underlying immunological processes. These results will inform future studies related to the safety and efficacy of any vaccines and may change our way of analyzing vaccine reactogenicity, leading to the development of safer yet efficacious vaccines and increased adherence to vaccines.

Limitations of the study

First, background information and adverse events were collected through a web-based questionnaire and a mobile app, so they have not been confirmed by experts and contain missing values. Compared to the electronic medical record obtained through interviews with physicians, there should be fluctuations and errors in individual answers. As shown in rank estimation using the masking approach, NTF can compensate for noise in the data. Nevertheless, the results obtained in this study will need to be validated using additional cohorts in the future to ensure generality and reliability. Secondly, we only assessed the antibody responses and did not assess other immune processes such as cellular and cytokine responses after vaccination. Antibodies are a major component of immune defense formed by vaccines, but it is also known that immunity induced by memory T cells and removal of infected cells by CD8 T cells also contribute to the defense against viral infection (Cox and Brokstad, 2020). The adverse reaction components that were not associated with the antibody titer in this study may be related to these other protective responses, so it is necessary to investigate the relationship with immunological parameters other than antibody titer in the future.

ETHICS

The study procedures were approved by Chiba University Ethics Committee (HS202101-03 and HS202104-01).

STAR★METHODS

Detailed methods are provided in the online version of this paper and include the following:

- KEY RESOURCES TABLE
- RESOURCE AVAILABILITY
  - Lead contact
  - Materials availability
  - Data and code availability
- EXPERIMENTAL MODEL AND SUBJECT DETAILS
  - Study subjects
- METHOD DETAILS
  - Data collection
  - Antibody response
  - Non-negative tensor factorization (NTF)
  - Non-negative matrix factorization (NMF)
  - Optimal number of tensor components
  - Machine learning classifier
- QUANTIFICATION AND STATISTICAL ANALYSIS

SUPPLEMENTAL INFORMATION

Supplemental information can be found online at https://doi.org/10.1016/j.isci.2022.105237.

ACKNOWLEDGMENTS

We thank all staff at Chiba University Hospital for supporting sample collection. This study was supported by a donation to Chiba University Hospital, the Future Medicine Founds at Chiba University, Japan Science and Technology Agency (JST) Moonshot R&D Grants (JPMJMS2025, to S.I., T.S., H.N. and E.K. and JPMJMS2021 to S.I.), a JST CREST Grant (JPMJCR20H4, to E.K.), a JST-Mirai (to S.I.), a JST PRESTO grant (JPMJPR1945 to K.T.), a MEXT KAKENHI (19K20406 to K.T.) and Japan Agency for Medical Research and Development (AMED) Grants (JP21wm0325007, JP20fk0108412, JP20fk0108413, JP21gm5010003, all to E.K.).

AUTHOR CONTRIBUTIONS

K.I., T.N., T.K., S.T., S.I., T.S., H.N., and E.K. participated in the design of the study. T.N., T.K., S.T., T.T., H.I., H.H., K.Y., and H.N. participated in data collection. K.I., T.K., S.T., N.Y., T.I., Y.G., N.O., K.T., H.N., and E.K. participated in data analyses. All the authors interpreted the data and participated in writing and critical review of the article and approved the final version.

DECLARATION OF INTERESTS

The authors have no competing interests to declare.

INCLUSION AND DIVERSITY

We worked to ensure gender balance in the recruitment of human subjects. We worked to ensure that the study questionnaires were prepared in an inclusive way.

Received: February 18, 2022
Revised: July 5, 2022
Accepted: September 22, 2022
Published: October 21, 2022

REFERENCES

Acar, E., Aykut-Bingol, C., Bingol, H., Bro, R., and Yener, B. (2007). Multiway analysis of epilepsy tensors. Bioinformatics *23*, i10–i18. https://doi.org/10.1093/bioinformatics/btm210.

Acar, E., Lawaetz, A.J., Rasmussen, M.A., and Bro, R. (2013). Structure-revealing data fusion model with applications in metabolomics. Annu. Int. Conf. IEEE Eng. Med. Biol. Soc. 6023–6026. https://doi.org/10.1109/EMBC.2013.6610925.

Baden, L.R., El Sahly, H.M., Essink, B., Kotloff, K., Frey, S., Novak, R., Diemert, D., Spector, S.A., Rouphael, N., Creech, C.B., et al. (2021). Efficacy and safety of the mRNA-1273 SARS-CoV-2 vaccine. N. Engl. J. Med. *384*, 403–416. https://doi.org/10.1056/NEJMoa2035389.

Batmanghelich, N., Dong, A., Taskar, B., and Davatzikos, C. (2011). Regularized tensor factorization for multi-modality medical image classification. Med. Image Comput. Comput. Assist. Interv. *14*, 17–24. https://doi.org/10.1007/978-3-642-23626-6_3.

Chang, J., Gerrish, S., Wang, C., Boyd-graber, J., and Blei, D. (2009). Reading tea leaves: how humans interpret topic models. In Advances in Neural Information Processing Systems, Y. Bengio, D. Schuurmans, J. Lafferty, C. Williams, and A. Culotta, eds. (Curran Associates, Inc.).

Cichocki, A., Zdunek, R., Phan, A.H., and Amari, S. (2009). Nonnegative Matrix and Tensor Factorizations: Applications to Exploratory Multi-Way Data Analysis and Blind Source Separation (John Wiley and Sons).

Cichocki, A., Cruces, S., and Amari, S.-I. (2011). Generalized alpha-beta divergences and their application to robust nonnegative matrix factorization. Entropy *13*, 134–170. https://doi.org/10.3390/e13010134.

Cooper, M.D., and Alder, M.N. (2006). The evolution of adaptive immune systems. Cell *124*, 815–822. https://doi.org/10.1016/j.cell.2006.02.001.

Cox, R.J., and Brokstad, K.A. (2020). Not just antibodies: B cells and T cells mediate immunity to COVID-19. Nat. Rev. Immunol. *20*, 581–582. https://doi.org/10.1038/s41577-020-00436-4.

Dagan, N., Barda, N., Kepten, E., Miron, O., Perchik, S., Katz, M.A., Hernán, M.A., Lipsitch, M., Reis, B., and Balicer, R.D. (2021). BNT162b2 mRNA Covid-19 vaccine in a nationwide mass vaccination setting. N. Engl. J. Med. *384*, 1412–1423. https://doi.org/10.1056/NEJMoa2101765.

Fanaee-T, H., and Gama, J. (2016). Tensor-based anomaly detection: an interdisciplinary survey. Knowl. Base Syst. *98*, 130–147. https://doi.org/10.1016/j.knosys.2016.01.027.

Févotte, C., Bertin, N., and Durrieu, J.L. (2009). Nonnegative matrix factorization with the Itakura-Saito divergence: With application to music analysis. Neural comput. *21*, 793–830.

Frenck, R.W., Jr., Klein, N.P., Kitchin, N., Gurtman, A., Absalon, J., Lockhart, S., Perez, J.L., Walter, E.B., Senders, S., Bailey, R., et al. (2021). Safety, immunogenicity, and efficacy of the BNT162b2 Covid-19 vaccine in adolescents. N. Engl. J. Med. *385*, 239–250. https://doi.org/10.1056/NEJMoa2107456.

Gaujoux, R., and Seoighe, C. (2010). A flexible R package for nonnegative matrix factorization. BMC Bioinf. *11*, 367. https://doi.org/10.1186/1471-2105-11-367.

Haas, E.J., Angulo, F.J., McLaughlin, J.M., Anis, E., Singer, S.R., Khan, F., Brooks, N., Smaja, M., Mircus, G., Pan, K., et al. (2021). Impact and effectiveness of mRNA BNT162b2 vaccine against SARS-CoV-2 infections and COVID-19 cases, hospitalisations, and deaths following a nationwide vaccination campaign in Israel: an observational study using national surveillance data. Lancet *397*, 1819–1829. https://doi.org/10.1016/S0140-6736(21)00947-8.

Hervé, C., Laupèze, B., Del Giudice, G., Didierlaurent, A.M., and Tavares Da Silva, F. (2019). The how's and what's of vaccine reactogenicity. NPJ Vaccines *4*, 39. https://doi.org/10.1038/s41541-019-0132-6.

Huang, Z., Dong, W., and Duan, H. (2015). A probabilistic topic model for clinical risk stratification from electronic health records. J. Biomed. Inform. *58*, 28–36. https://doi.org/10.1016/j.jbi.2015.09.005.

Ji, S. (2011). Computational network analysis of the anatomical and genetic organizations in the mouse brain. Bioinformatics *27*, 3293–3299. https://doi.org/10.1093/bioinformatics/btr558.

Kageyama, T., Ikeda, K., Tanaka, S., Taniguchi, T., Igari, H., Onouchi, Y., Kaneda, A., Matsushita, K., Hanaoka, H., Nakada, T.-A., et al. (2021). Antibody responses to BNT162b2 mRNA COVID-19 vaccine and their predictors among healthcare workers in a tertiary referral hospital in Japan. Clin. Microbiol. Infect. *27*, 1861.e1–1861.e5. https://doi.org/10.1016/j.cmi.2021.07.042.

Kossaifi, J., Panagakis, Y., Anandkumar, A., and Pantic, M. (2016). Tensorly: tensor learning in python. Preprint at arXiv. https://doi.org/10.48550/arXiv.1610.09555.

Lau, J.H., Newman, D., and Baldwin, T. (2014). Machine reading tea leaves: automatically evaluating topic coherence and topic model quality. In Proceedings of the 14th Conference of the European Chapter of the Association for Computational Linguistics, pp. 530–539. https://doi.org/10.3115/v1/E14-1056.

Lauvau, G., and Goriely, S. (2016). Memory CD8+ T cells: orchestrators and key players of innate immunity? PLoS Pathog. *12*, e1005722. https://doi.org/10.1371/journal.ppat.1005722.

Lin, X., and Boutros, P.C. (2020). Optimization and expansion of non-negative matrix factorization. BMC Bioinf. *21*, 7. https://doi.org/10.1186/s12859-019-3312-5.

Lu, H.-M., Wei, C.-P., and Hsiao, F.-Y. (2016). Modeling healthcare data using multiple-channel latent Dirichlet allocation. J. Biomed. Inform. *60*, 210–223. https://doi.org/10.1016/j.jbi.2016.02.003.

Luo, Y., Wang, F., and Szolovits, P. (2017). Tensor factorization toward precision medicine. Brief. Bioinform. *18*, 511–514. https://doi.org/10.1093/bib/bbw026.

Newman, D., Lau, J.H., Grieser, K., and Baldwin, T. (2010). Automatic evaluation of topic coherence. In Human Language Technologies: The 2010 Annual Conference of the North American Chapter of the Association for Computational Linguistics, pp. 100–108.

Palm, N.W., and Medzhitov, R. (2007). Not so fast: adaptive suppression of innate immunity. Nat. Med. *13*, 1142–1144. https://doi.org/10.1038/nm1007-1142b.

Parish, I.A., and Kaech, S.M. (2009). Diversity in CD8+ T cell differentiation. Curr. Opin. Immunol. *21*, 291–297. https://doi.org/10.1016/j.coi.2009.05.008.

Pedregosa, F., Varoquaux, G., Gramfort, A., Michel, V., Thirion, B., Grisel, O., Blondel, M., Prettenhofer, P., Weiss, R., Dubourg, V., et al. (2011). Scikit-learn: machine learning in Python. J. Mach. Learn. Res. *12*, 2825–2830.

Perros, I., Papalexakis, E.E., Vuduc, R., Searles, E., and Sun, J. (2019). Temporal phenotyping of medically complex children via PARAFAC2 tensor factorization. J. Biomed. Inform. *93*, 103125. https://doi.org/10.1016/j.jbi.2019.103125.

Perry, O.P. (2009). Cross-validation for Unsupervised Learning. Ph.D. thesis (Stanford University). https://doi.org/10.48550/arXiv.0909.3052.

Pivovarov, R., Perotte, A.J., Grave, E., Angiolillo, J., Wiggins, C.H., and Elhadad, N. (2015). Learning probabilistic phenotypes from heterogeneous EHR data. J. Biomed. Inform. *58*, 156–165. https://doi.org/10.1016/j.jbi.2015.10.001.

Polack, F.P., Thomas, S.J., Kitchin, N., Absalon, J., Gurtman, A., Lockhart, S., Perez, J.L., Pérez Marc, G., Moreira, E.D., Zerbini, C., et al. (2020). Safety and efficacy of the BNT162b2 mRNA Covid-19 vaccine. N. Engl. J. Med. *383*, 2603–2615. https://doi.org/10.1056/NEJMoa2034577.

Ren, K., and Dubner, R. (2010). Interactions between the immune and nervous systems in pain. Nat. Med. *16*, 1267–1276. https://doi.org/10.1038/nm.2234.

Robin, X., Turck, N., Hainard, A., Tiberti, N., Lisacek, F., Sanchez, J.C., and Müller, M. (2011). pROC: an open-source package for R and S+ to analyze and compare ROC curves. BMC Bioinform. *12*, 1–8.

Roy, S., Homayouni, R., Berry, M.W., and Puretskiy, A.A. (2014). Nonnegative tensor factorization of biomedical literature for analysis of genomic data. In Data Mining for Service, K. Yada, ed. (Springer Berlin Heidelberg), pp. 97–110.

Sadoff, J., Gray, G., Vandebosch, A., Cárdenas, V., Shukarev, G., Grinsztejn, B., Goepfert, P.A., Truyers, C., Fennema, H., Spiessens, B., et al. (2021). Safety and efficacy of single-dose Ad26.COV2.S vaccine against Covid-19. N. Engl. J. Med. *384*, 2187–2201. https://doi.org/10.1056/NEJMoa2101544.

Saper, C.B., Romanovsky, A.A., and Scammell, T.E. (2012). Neural circuitry engaged by prostaglandins during the sickness syndrome. Nat. Neurosci. *15*, 1088–1095. https://doi.org/10.1038/nn.3159.

Shashua, A., and Hazan, T. (2005). Non-negative tensor factorization with applications to statistics and computer vision. In Proceedings of the 22nd International Conference on Machine Learning (Association for Computing Machinery), pp. 792–799.

Smyth, G., Hu, Y., Dunn, P., Phipson, B., Chen, Y., and Smyth, M.G. (2021). Package 'statmod'. https://cran.r-project.org/web/packages/statmod/index.html.

Stekhoven, D.J., and Bühlmann, P. (2012). MissForest—non-parametric missing value imputation for mixed-type data. Bioinformatics *28*, 112–118.

Stevens, K., Kegelmeyer, P., Andrzejewski, D., and Buttler, D. (2012). Exploring topic coherence over many models and many topics. In Proceedings of the 2012 Joint Conference on Empirical Methods in Natural Language Processing and Computational Natural Language Learning, pp. 952–961.

Vasilache, A.M., Qian, H., and Blomqvist, A. (2015). Immune challenge by intraperitoneal administration of lipopolysaccharide directs gene expression in distinct blood-brain barrier cells toward enhanced prostaglandin E(2) signaling. Brain Behav. Immun. *48*, 31–41. https://doi.org/10.1016/j.bbi.2015.02.003.

Vincent, P., Larochelle, H., Bengio, Y., and Manzagol, P.-A. (2008). Extracting and composing robust features with denoising autoencoders. In Proceedings of the 25th International Conference on Machine Learning (Association for Computing Machinery), pp. 1096–1103.

Voysey, M., Clemens, S.A.C., Madhi, S.A., Weckx, L.Y., Folegatti, P.M., Aley, P.K., Angus, B., Baillie, V.L., Barnabas, S.L., Bhorat, Q.E., et al. (2021). Safety and efficacy of the ChAdOx1 nCoV-19 vaccine (AZD1222) against SARS-CoV-2: an interim analysis of four randomised controlled trials in Brazil, South Africa, and the UK. Lancet *397*, 99–111. https://doi.org/10.1016/S0140-6736(20)32661-1.

Wood, S., and Wood, M.S. (2015). Package 'mgcv'. R Package Version, 1, p. 729.

Wood, S. (2018). Mixed GAM computation vehicle with automatic smoothness estimation. R Package Version *1*, 8–12.

Wu, X., Shi, B., Dong, Y., Huang, C., and Chawla, N.V. (2019). Neural tensor factorization for temporal interaction learning. In Proceedings of the Twelfth ACM international conference on web search and data mining, pp. 537–545.

Yamada, M., Nakada, T.-A., Nakao, S., Hira, E., Shinozaki, K., Kawaguchi, R., Mizushima, Y., and Matsuoka, T. (2019). Novel information and communication technology system to improve surge capacity and information management in the initial hospital response to major incidents. Am. J. Emerg. Med. *37*, 351–355. https://doi.org/10.1016/j.ajem.2018.06.007.

Zhao, J., Feng, Q., Wu, P., Warner, J.L., Denny, J.C., and Wei, W.-Q. (2019a). Using topic modeling via non-negative matrix factorization to identify relationships between genetic variants and disease phenotypes: a case study of Lipoprotein(a) (LPA). PLoS One *14*, e0212112. https://doi.org/10.1371/journal.pone.0212112.

Zhao, J., Zhang, Y., Schlueter, D.J., Wu, P., Eric Kerchberger, V., Trent Rosenbloom, S., Wells, Q.S., Feng, Q., Denny, J.C., and Wei, W.-Q. (2019b). Detecting time-evolving phenotypic topics via tensor factorization on electronic health records: cardiovascular disease case study. J. Biomed. Inform. *98*, 103270. https://doi.org/10.1016/j.jbi.2019.103270.

STAR★METHODS

KEY RESOURCES TABLE

REAGENT or RESOURCE	SOURCE	IDENTIFIER
Software and algorithms		
R-4.0.2	R Foundation for Statistical Computing	https://www.r-project.org/
Python-3.8.5	Python Software Foundation	https://www.python.org/
TensorLy-0.6.0	Kossaifi et al., 2016	http://tensorly.org/stable/index.html
scikit-learn-0.23.2	Pedregosa et al., 2011	https://scikit-learn.org/stable/index.html
pROC-1.17.0.1	Robin et al., 2021	https://cran.r-project.org/web/packages/pROC/index.html
missForest-1.4	Stekhoven and Bühlmann, 2012	https://cran.r-project.org/web/packages/missForest/index.html
statmod-1.4.35	Smyth et al., 2021	https://cran.r-project.org/web/packages/statmod/index.html
mgcv-1.8.34	Wood and Wood, 2015	https://cran.r-project.org/web/packages/mgcv/index.html

RESOURCE AVAILABILITY

Lead contact

Further information and requests for resources should be directed to and will be fulfilled by the lead contact, Eiryo Kawakami (eiryo.kawakami@chiba-u.jp).

Materials availability

This study did not generate new unique reagents.

Data and code availability

Data reported in this paper will be shared by the lead contact upon request. The raw vaccine adverse reaction datasets and source-code used to perform NTF are publicly available at https://github.com/github.com/eiryo-kawakami/Vaccine_Tensor_2022_code. Any additional information required to reanalyze the data reported in this paper is available from the lead contact upon request.

EXPERIMENTAL MODEL AND SUBJECT DETAILS

Study subjects

We recruited healthcare workers who were receiving the BNT162b2 (Pfizer, Inc., and BioNTech) in the vaccination program of Chiba University Hospital (Kageyama et al., 2021). Out of 2,838 employees in Chiba University Hospital, 2,549 received at least one dose of BNT162b2 mRNA COVID-19 vaccine (30 μg) from March 3rd to April 9th, 2021. The adverse-reaction information was obtained for 1,774 individuals who received two doses, whose median age was 38 (interquartile range 30–48) with 1,168 (65.8%) being women. All participants gave written informed consent before undergoing any study procedures.

METHOD DETAILS

Data collection

Background information was collected with web-based questionnaires. Information on adverse reactions was collected every day using a smartphone/web-based platform (Yamada et al., 2019) from the vaccination day (day 0) to the 14th day after vaccination (day 14) for both doses. On the day of inoculation (day 0), subjects were asked to respond to each of the 18 symptoms to assess reactions immediately after inoculation (Table S1). In the questionnaire after day 1, subjects were asked to respond to each of the 12 symptoms with a score from 0 (no symptoms) to 3 (severe symptoms), corresponding to the degree of symptoms (Table S2). We analyzed the adverse-reaction data from day 1 to day 7 after each dose because few adverse

reactions remained and the rates of response to the questionnaires were lower at day 8 or after (Figure S1). We also focused on 1,516 subjects who had a missing response rate of less than 30%.

Antibody response

Blood samples were obtained 2–5 weeks after the 2nd dose of vaccination. Antibody titers were determined using Elecsys® Anti-SARS-CoV-2S on Cobas 8000 e801 module (Roche Diagnostics, Rotkreuz, Switzerland).

Non-negative tensor factorization (NTF)

The time-series data for adverse reactions can be represented as a third-order tensor, $\mathcal{X} \in \mathbb{R}^{S \times T \times N}$, where S is the number of symptoms, T is the number of observation time points, and N is the number of subjects. For the adverse-reaction data in this study, $S = 12$, $T = 14$, and $N = 1,516$ and all the elements of $\mathcal{X}$ were non-negative. We used canonical polyadic (CP) decomposition to represent the third-order tensor as a product of lower-dimensional elements and reveal the latent structures. Since all values of the original third-order tensor in this study are greater than or equal to zero, i.e., non-negative, we used non-negative PARAFAC (Shashua and Hazan, 2005), a type of CP decomposition implemented in a Python library *Tensorly* (Kossaifi et al., 2016). The non-negative PARAFAC decomposition function *non_negative_parafac* aims to obtain r components that approximate the original third-order tensor $\mathcal{X}$ as:

$$min \left\| \mathcal{X} - \widehat{\mathcal{X}} \right\|_F^2,$$

$$\text{with } \widehat{\mathcal{X}} = \sum_{r=1}^{R} \boldsymbol{\lambda}_r \, \boldsymbol{a}_r \circ \boldsymbol{b}_r \circ \boldsymbol{c}$$

$$= \Lambda \times_1 A \times_2 B \times_3 C$$

$$subject\ to: \Lambda,\ A,\ B,\ C \geq 0,$$

where Λ is a third-order diagonal tensor whose r-th diagonal element $\Lambda_{rrr} = \boldsymbol{\lambda}_r$, $A = [a_1, a_2, \ldots, a_R] \in \mathbb{R}_+^{S \times R}$, $B = [b_1, b_2, \ldots, b_R] \in \mathbb{R}_+^{T \times R}$, and $C = [c_1, c_2, \ldots, c_R] \in \mathbb{R}_+^{N \times R}$ denote factor matrices. $\left\| \mathcal{X} - \widehat{\mathcal{X}} \right\|_F^2$ is the squared Frobenius norm to evaluate the reconstruction error between the original tensor $\mathcal{X}$ and the reconstructed tensor $\widehat{\mathcal{X}}$, $\circ$ denotes the outer product of two vectors, and $\times_m$ denote the m-mode product of a tensor by a matrix (m =1, 2, or 3, Cichocki et al., 2009). The initial values of A, B, and C are filled with random values drawn from the uniform distribution taking values in the range 0 to 1. In each iteration step, $\mathcal{X}$ is matricized (unfolded) in the m-mode and the multiplicative update rule is performed to update A, B, and C. In the initialization and each iteration step, the column vectors of A, B, and C are normalized so that their L2-norms are equal to 1. To avoid division by zero or unstable calculation, the small values less than machine epsilon (ε) were replaced by ε in the initialization and the last part of each iteration. The convergence is evaluated by two stopping criteria: the tolerance for reconstruction error variation and the maximum number of iterations. If at least one of the criteria is met (the reconstruction error variation is less than tolerance or the number of iterations exceed the maximum), the calculation is considered to be converged and stops. We used the tolerance (*tol* parameter in *non_negative_parafac* function) of 10^{-6} and the maximum number of iterations (*n_iter_max* parameter in *non_negative_parafac* function) of 1,000 for the rank optimization and 5,000 for the final decomposition. The mask property implemented in *non_negative_parafac* function was applied on the missing elements in the original tensor to exclude them from the NTF fitting.

Non-negative matrix factorization (NMF)

The adverse-reaction data at each time point is represented as a two-order matrix, $X \in \mathbb{R}^{N \times S}$, where S is the number of symptoms and N is the number of subjects. The NMF aims to approximate the matrix X as an inner product of two matrices W and H as:

$$min \left\| X - WH \right\|_F^2,$$

$$subject\ to: W,\ H \geq 0,$$

where $W \in \mathbb{R}^{N \times K}$ and $H \in \mathbb{R}^{K \times S}$. To compare NMF with NTF under the same conditions as possible, we used *non_negative_parafac* function implemented in Python library *TensorLy*. Since matrix can also be viewed as a second-order tensor, applying non-negative PARAFAC to matrices is equivalent to NMF. Thus, we

performed NMF under the same conditions of initialization, normalization, update rule, avoiding division-by-zero errors, and stopping criteria as for NTF.

Optimal number of tensor components

We adopted a masking approach to determine the optimal number of components in NTF, which has been previously proposed for rank optimization of NMF (Lin and Boutros, 2020). The masking approach determines an optimal rank to give the smallest error in imputing the masked elements, which is also known as "denoising" or "unsupervised cross validation" in machine learning context (Vincent et al., 2008; Perry, 2009). This assumes that the reconstruction performance for the masked elements should be maximized at the optimal rank that properly captures the latent structure of the data. In the NTF, some non-zero elements of the original data were randomly masked to obtain the noisy data. The reconstruction error is calculated as the mean squared error (MSE) only for the masked elements. In this study, the median reconstruction error, obtained from 50 independent decompositions for each rank, was used as the optimization metric.

Machine learning classifier

Random forest (RF) classifiers were applied to predict tensor component score for subjects and post-vaccination anti-SARS-CoV-2S antibody titers. To account for the nonlinearity and interactions between explanatory and objective variables, we formulated the predictions as binary classification problems, with the objective variables binarized by thresholds. The RF is an ensemble machine learning method that constructs multiple decision trees with randomly selected dataset using bootstrap sampling. We used *RandomRorestClassifier* function in Python package *scikit-learn*. *GridSearchCV* function in the *scikit-learn* package was applied to optimize the hyperparameters of the RF classifiers. The performance of each RF classifier was evaluated using an area under the receiver operating characteristic (ROC) curve using R package *pROC*. Permutation importance was used to assess the contribution of explanatory variables to prediction, which randomly permutes a variable across subjects to evaluate the effect on the performance of the machine learning model, in this case, the AUC. Missing values in the background factors were imputed using the *missForest* package in R.

QUANTIFICATION AND STATISTICAL ANALYSIS

The correlations between decomposed components and acute reactions were analyzed using Spearman's rank correlation. The associations with background factors were assessed with a generalized linear model assuming a Tweedie distribution for tensor components to accommodate their zero-inflated nature. We used the *glm()* function in the R package stats and *tweedie()* function in the R package *statmod*. In the association analysis between tensor components and antibody titers, the generalized additive model implemented in R package *mgcv* (Wood, 2018) was used with covariates including interval to test, age, interval between the 1st and 2nd inoculation, alcohol, use of immunosuppressant, use of glucocorticoid, use of anti-allergic drug, and post COVID-19 infection. To account for the nonlinear effects of interval to test and age, they were added as smooth terms to the model:

$$\begin{aligned} \textit{Antibody Titer} \sim\ & \alpha + \beta 1\ \textit{tensor component subject score} + s(\textit{interval to test}) + s(\textit{age}) \\ & + \beta 2\ \textit{inoculation interval} + \beta 3\ \textit{alcohol} + \beta 4\ \textit{immunosuppressant} \\ & + \beta 5\ \textit{glucocorticoid} + \beta 6\ \textit{anti allergic drug} + \beta 7\ \textit{COVID19 infection} + \epsilon \end{aligned}$$

Plots in Figure 4F show antibody titers adjusted to the standard conditions of interval to test (days) = 21, inoculation interval (days) = 21, age (year-old) = 40, alcohol = none, immunosuppressant = none, glucocorticoid = none, anti-allergic drug = none, and post COVID-19 infection = none. A two-sided p-value < 0.05, false discovery rate (FDR)-corrected, was considered statistically significant.